ACS APPLIED MATERIALS & INTERFACES

www.acsami.org

Research Article

Multivalent Supramolecular Assembly Based on a Triphenylamine Derivative for Near-Infrared Lysosome Targeted Imaging

Jie Yu, Hui Wang, Xianyin Dai, Yong Chen, and Yu Liu*

Cite This: *ACS Appl. Mater. Interfaces* 2022, 14, 4417−4422

Read Online

ACCESS | Metrics & More | Article Recommendations | Supporting Information

ABSTRACT: Near-infrared (NIR) targeted cell imaging has become a research hotspot due to the advantages of deeper tissue penetration, minimal interference from the background signals, and lower light damage. Herein, we report a multivalent supramolecular aggregate with NIR fluorescence emission, which was fabricated from triphenylamine derivatives (TPAs), cucurbit[8]uril (CB[8]), Si-rhodamine (SiR), and hyaluronic acid (HA). Interestingly, possessing a rigid luminescent core and cationic phenylpyridinium units linked by flexible alkyl chains, the tripaddle hexacationic TPA could bind with CB[8] at a 2:3 stoichiometric ratio to form a network-like multivalent assembly with enhanced red luminescence. Such organic two-dimensional network-like aggregate further co-assembled with the energy acceptor SiR and cancer cell targeting agent HA, leading to nanoparticles with NIR emission at 675 nm via an intermolecular energy transfer pathway. Furthermore, the obtained multivalent supramolecular aggregate was successfully applied in lysosome targeted imaging toward A549 cancer cells, which provides a convenient strategy for NIR targeted cell imaging.

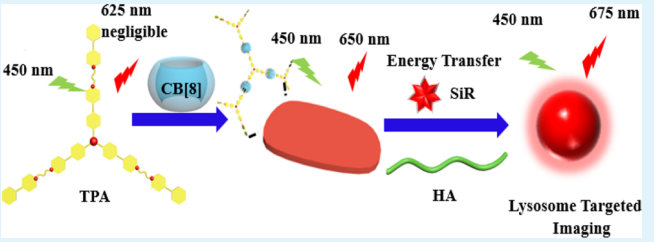

KEYWORDS: *multivalent supramolecular assembly, triphenylamine, cucurbit[8]uril, hyaluronic acid, near-infrared imaging*

INTRODUCTION

Recently, possessing fluorescence emission in the range of 650−900 nm, near-infrared dyes have become a research hotspot in biological imaging, mainly because NIR fluorescence emission possesses various salient advantages including less photo-induced damage to living cells,[1] deeper tissue penetration,[2] and minimum interference from biomolecule signals.[3,4] At present, it still remains a challenge to fabricate a targeted NIR platform with good water solubility, biocompatibility, and excellent luminescence properties, and tedious and complex synthesis work is inevitable. On the other hand, multivalent supramolecular assembly provides an effective approach to build versatile systems.[5−10] Particularly, multivalent supramolecular assembly based on macrocyclic compounds could effectively induce enhanced luminescence properties of fluorophores and further expand the application of artificial nanomaterials in the areas of cell imaging and luminescence materials.[11,12]

Among the various macrocyclic compounds, cucurbit[8]uril possesses a hydrophobic inner cavity and rigid structure that could bond two guest molecules,[13,14] which are beneficial to the formation of stable complexes[15−17] and also extend the conjugation of the assembly.[18,19] Recently, the Scherman group found that CB[8] could bind with 1-(*p*-tolyl)pyridin-1-ium modified 2,6-anthracenyl derivatives to form pseudo[2,3]-rotaxanes with NIR fluorescence emission at 657 nm.[20] Park et al. reported that red luminescent supramolecular polymers were facilely constructed by CB[8] and cyanostilbenes.[21] Tian et al. reported that cucurbituril (CB) interacted with peptide modified Au nanoclusters (AuNCs) and then enhanced the red phosphorescence emission of AuNCs.[22] We reported that CB[8] mediated a vinyl pyridine salt modified anthracene or tetraphenylethene derivative to form NIR emission linear[23] and nanosquare-shaped[24] assemblies, respectively. Most of the reported NIR supramolecular systems based on CB are linear or particle-shaped assemblies; however, these researches are rarely about network-like NIR conjugates. In this work, an NIR luminescent multivalent supramolecular aggregate was fabricated from triphenylamine derivatives (TPAs), CB[8], Si-rhodamine (SiR), and hyaluronic acid (HA), and it showed a lysosome targeted imaging ability (Scheme 1). The hexacationic TPA not only has a rigid luminescent core but also is attached with a cationic phenylpyridinium unit linked by flexible alkyl chains. Thus, the tripaddle hexacationic TPA could act as a cross-link center to bind with CB[8] in a 2:3 (TPA/CB[8]) complexation stoichiometry via host−guest interaction to form a two-dimensional network-like aggregate emitting red luminescence. Moreover, the energy acceptor SiR was successfully introduced to the TPA/CB[8] conjugate by

Received: October 12, 2021
Accepted: December 29, 2021
Published: January 10, 2022

Scheme 1. Schematic Illustration of a Multivalent Supramolecular Aggregate with NIR Emission

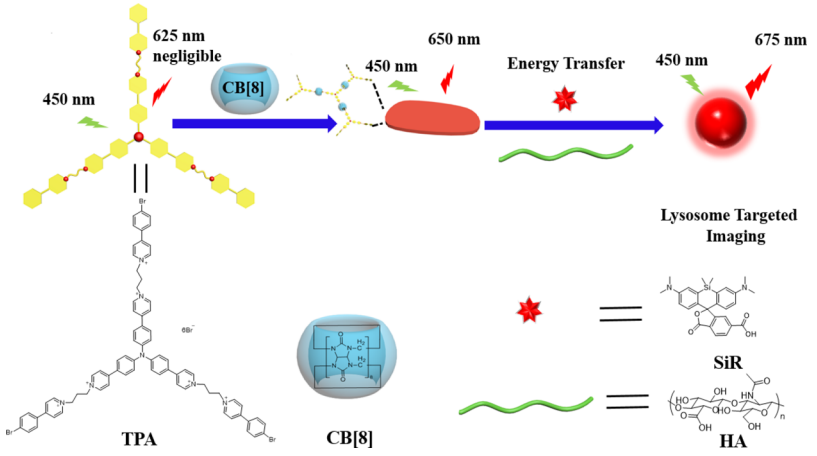

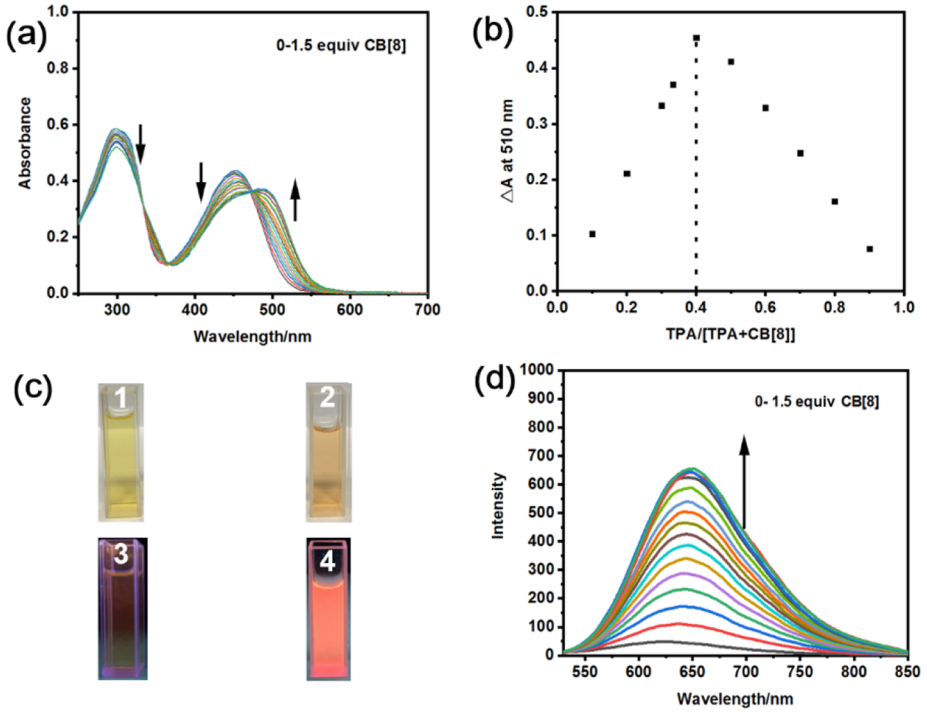

Figure 1. (a) Absorption spectra of TPA in the presence of different ratios of CB[8] at 25 °C ([TPA] = 0.01 mM). (b) Job plot of TPA/CB[8] complexation in an aqueous solution (absorption changes were recorded at 510 nm for TPA ([TPA] = [CB[8]] = 0.05 mM)). (c) Photographs of TPA and TPA/CB[8] under visible light (1 and 2, respectively) or UV light (365 nm) (3 and 4, respectively). (d) Fluorescence spectra of TPA in the presence of different ratios of CB[8] in an aqueous solution at 25 °C ([TPA] = 0.01 mM, λ_{ex} = 450 nm).

electrostatic interaction that then resulted in a bathochromic shift at 675 nm. Furthermore, this multi-cation network-like aggregate further transformed into nanoparticles through co-assembly with hyaluronic acid, exhibiting further enhanced fluorescence emission. Importantly, CB[8] could induce TPA homodimerization and then further co-assembly to form nanoparticles, which not only could increase the intensity of fluorescence but also present efficient energy transfer. The two-step multivalent supramolecular aggregate with NIR emission was also successfully applied in lysosome targeted imaging for A549 cancer cells. Therefore, by the strategy of supramolecular assembly, a targeted near-infrared supramolecular probe was successfully fabricated and also provided a facile and convenient method to investigate the interaction process of fluorophores and organelles in cells.[23,25]

EXPERIMENTAL SECTION

Materials and Methods. The regents and solvents were commercially available. The purification and characterization of compounds, UV−vis/fluorescence spectra, and morphology of aggregates were performed according to a previously reported method.[26] Cell images were captured on a Leica S8 microscope and Olympus FV1000 laser scanning confocal microscope.

The Procedure for the Synthesis of TPA. 4-(4-Bromophenyl)-pyridine (350 mg, 1.50 mmol) and compound 2 (270 mg, 0.25 mmol) were added to dry DMF. The solution was stirred at 90 °C for 1 day under argon protection. After that, the solution was poured into THF and the resulting red solid was obtained by filtration, further washed by dry THF three times, and then dried under vacuum, yielding 0.34 g of solid.

Cell Imaging Experiments. The cell imaging experiments were performed according to a previously reported method.[12] Commer-

https://doi.org/10.1021/acsami.1c19698
ACS Appl. Mater. Interfaces 2022, 14, 4417−4422

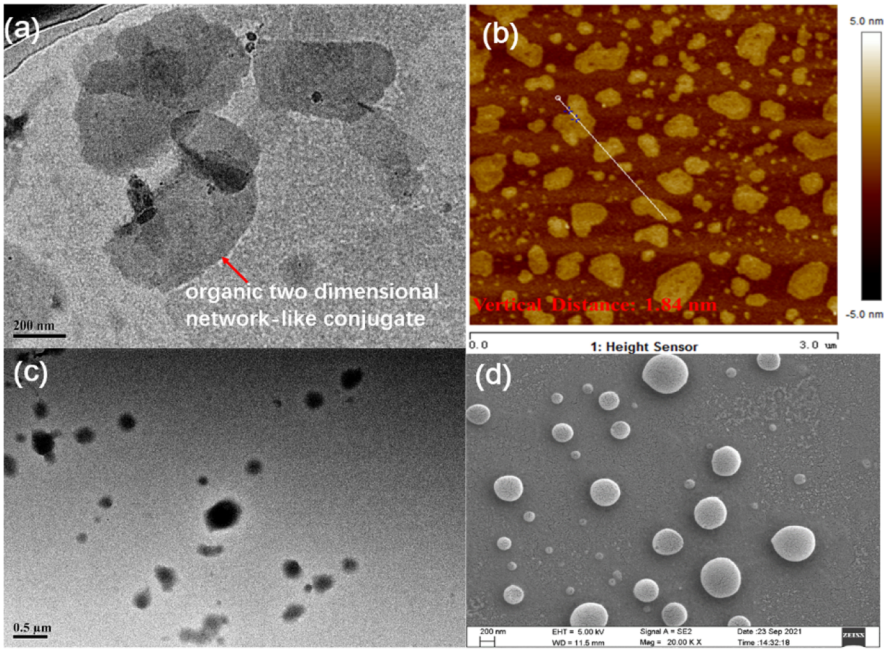

Figure 2. (a) TEM and (b) AFM image of TPA/CB[8]. (c) TEM and (d) SEM image of TPA/CB[8]/SiR/HA.

cially available A549 cells were purchased from the Cell Resource Center, China Academy of Medical Science Beijing, China, and then precultured for 24 h. After incubation with TPA/CB[8]/SiR/HA for 4 h, DAPI (the nuclei dye), LysoTracker Green (a lysosome tracker), or MitoTracker Green (a mitochondrion tracker) was also added to cells, respectively, which were washed three times with PBS and then examined by confocal laser scanning microscopy.

RESULTS AND DISCUSSION

As shown in Scheme S1, triphenylamine derivative 1 was synthesized via the reaction of tris(4-bromophenyl)amine with pyridine-4-boronic acid. Subsequently, compound 1 reacted with an excess mount of 1,3-dibromopropane to give the intermediate 2. Finally, 4-(4-bromophenyl)pyridine reacted with compound 2 in anhydrous DMF for 24 h under argon to give TPA. In Figures S1−S3, the obtained guest compound TPA was identified by NMR and MS studies.

The obtained guest TPA molecule not only has a rigid luminescent core but also attached with three positively charged phenylpyridinium units linked by flexible alkyl chains. CB[8] with a large hydrophobic inner cavity could include the aromatic parts of phenylpyridinium derivatives and then give the complex at a 1:2 stoichiometric ratio.[13] First, the bonding behavior between TPA and CB[8] was explored by UV−vis spectroscopy. Figure 1a shows that after the addition of 1.5 equiv CB[8], the UV absorption of TPA at 450 nm gave a 45 nm bathochromic shift accompanied by the signals at 300 nm or 450 nm decreased, dash yellowed TPA solution changed to sight brown (Figure 1c), which may be ascribed to the positively charged phenylpyridinium units of TPA were included by host to give complexes. Subsequently, Job plot data exhibited that the maximum number was 0.4, manifesting that TPA could bind with CB[8] at a 2:3 ratio (Figure 1b).

Subsequently, the homodimerization of TPA and CB[8] was also investigated by NMR experiments. Judging from the cross-peaks in the two-dimensional NMR result (Figure S4), the protons of H_{a-k} were assigned to the corresponding peaks. The protons of the 4-bromophenyl ring (H_a and H_b) showed large upfield shifts of $\Delta\delta$ =1.05 ppm (7.70 to 6.65 ppm) after the addition of CB[8] (Figure S5), indicating that the 4-bromophenyl ring was deeply included by the cavity of host compounds. The pyridinium units ($H_{c,d}$) also exhibited 0.17 and 0.51 ppm upfield shifts, respectively. The 4-bromophenyl ring ($H_{a,b}$) presented a dramatic peak shift and shifted much more than the pyridinium moiety ($H_{c,d}$), which may be due to the inner cavity of host compounds providing a shielding effect. Furthermore, according to the ROESY spectra of TPA/CB[8] in D_2O (Figure S6), the phenyl protons of TPA ($H_{a,b}$) showed multiple cross-peaks with CB[8], which manifested the 4-(4-bromophenyl)pyridine units of TPA in host cavities. From the above experiment results, we preliminarily speculated that TPA/CB[8] may be able to form more extended supramolecular conjugates. The morphology of the TPA/CB[8] supramolecular aggregate was also investigated by the TEM experiment. There were two-dimensional network-like nanostructures found in Figure 2a. Subsequently, this aggregate was also investigated by the AFM experiment (Figure 2b), giving a height of about 1.84 nm, corresponding to the diameter of CB[8].[13] The TPA/CB[8] conjugate solution exhibited a light path (Figure S7). DLS data showed that the aggregate with a hydrodynamic diameter range of 30−60 nm was the majority component; meanwhile, a few conjugates about 290−680 nm in diameter were also found in this system (Figure S8). Furthermore, the zeta potential value of the TPA/CB[8] conjugate was positive (26 mV), indicating that positive charges are distributed on the surface of conjugates (Figure S9). On the basis of the above evidence, we can reasonably speculate that TPA/CB[8] could assemble to form extended supramolecular conjugates, and a possible assembling mode was proposed in Scheme 1.

Fluorescence spectrum experiments were also performed to investigate the luminescence properties of multivalent conjugates. TPA exhibited a negligible fluorescence emission (Figure 1c); however, after addition of the host, the maximum emission peak not only bathochromic shift 25 nm reach to NIR region but also the fluorescence intensity greatly increased (Figure 1d). Furthermore, the quantum yield of TPA was also

https://doi.org/10.1021/acsami.1c19698
ACS Appl. Mater. Interfaces 2022, 14, 4417−4422

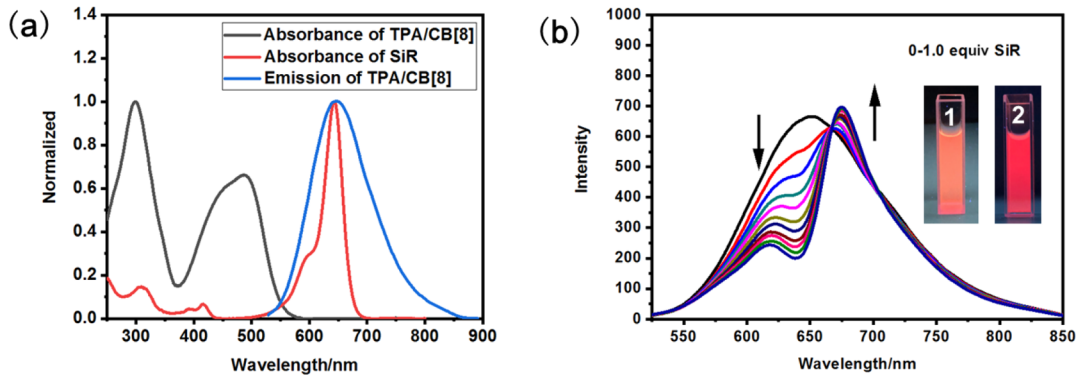

Figure 3. (a) Normalized absorption spectrum of TPA/CB[8] or SiR, and emission spectrum of TPA/CB[8]. (b) Fluorescence emission spectra of TPA/CB[8] in the presence of different ratios of SiR ([TPA] = 0.01 mM, [CB[8]] = 0.015 mM, λ_{ex} = 450 nm). Inset: photographs of TPA/CB[8] and TPA/CB[8]/SiR under UV light (365 nm) (1 and 2, respectively).

increased from 0.91 to 3.28%. This luminescence enhancement phenomenon was probably due to the fact that the cationic 4-(4-bromophenyl) pyridine groups of TPA were included by CB[8] to form stable extended supramolecular aggregates and then greatly restricted the movement of guests. The maximum emission peak of the multivalent supramolecular conjugate reaches 650 nm, which may be suitable for the study of excited energy transfer from the conjugate to SiR. In Figure 3a, the emission spectrum of TPA/CB[8] overlapped with the absorption spectrum of SiR, indicating that efficient excited energy might transfer from TPA/CB[8] to SiR. Subsequently, the energy transfer process between TPA/CB[8] and SiR was also identified by fluorescence titration results. In the presence of different amounts of SiR (Figure 3b), the fluorescence of TPA/CB[8] was gradually decreased; meanwhile, red luminescence from the acceptor was also present in this system. Furthermore, in this TPA/CB[8]/SiR conjugate, the energy transfer efficiency from TPA/CB[8] to SiR was up to 69%. Although the fluorescence emission of SiR or SiR/TPA systems was also observed under the same experiment condition (Figures S10−S11), the fluorescence intensity of TPA/CB[8]/SiR was much more higher than that of the control groups, indicating that the red luminescence emission at 675 nm was largely ascribed to SiR accepting the energy from TPA/CB[8]. The fluorescence lifetime of this conjugate showed no obvious change in the presence of 1.0 equiv SiR (Figure S12, from 1.61 to 1.60 ns), indicating that the energy transfer from TPA/CB[8] to SiR goes through the radiative energy transfer mechanism. SiR has two carboxyl groups with negative charges and a quaternary ammonium group with a positive charge after ring opening. Thus, SiR could be introduced into the cationic TPA/CB[8] via electrostatic interaction. Furthermore, TPA/CB[8]/SiR had a network-like morphology, and then energy dispersive X-ray spectroscopy (EDX) further confirmed that SiR was loaded to the conjugates (Figure S13).

According to previous reports, the artificial conjugates will transform to be more ordered and compact assemblies through secondary assembly.[22−24] Thus, hyaluronic acid (HA), a kind of negatively charged polysaccharide and cancer cell targeting agent,[27,28] was introduced into this system by the co-assembly with TPA/CB[8]/SiR via electrostatic interaction. Interestingly, the fluorescence emission of this system was gradually enhanced upon the addition of HA (Figure S14), which may be ascribed to the co-assembly of HA with TPA/CB[8]/SiR to form a compact assembly. This factor further restricts the movement of TPA/CB[8]/SiR[12] and then benefits NIR luminescence emission. As control experiments, the fluorescence emission of TPA/SiR was also increased in the presence of HA; however, the fluorescence intensity of TPA/SiR/HA was obviously weaker than that of TPA/CB[8]/SiR/HA (Figure S16). On the other hand, the fluorescence spectra of SiR without no obvious change was observed in the fluorescence spectra of SiR after the addition of HA (Figure S11). These results jointly manifested that both HA and CB[8] were indispensable to the fluorescence enhancement of this multivalent supramolecular aggregate. Subsequently, DLS, zeta potential, TEM, and SEM experiments were performed to study the co-assembly behavior of this conjugate and HA. In the TEM experiment, there were spherical nanoparticles about 100−500 nm in diameter as shown in Figure 2c; SEM images also gave a similar morphology (Figure 2d). Moreover, DLS results (Figure S8) showed that the aggregates with a hydrodynamic diameter range of 170−240 nm were the majority component; meanwhile, a few aggregates about 380−530 nm in diameter also existed in the solution, which basically coincide with above observed nanoparticles. This multivalent aggregate gave a negative surface potential value (−2.5 mV, Figure S9), indicating that anionic HA was distributed on the surface of conjugates. Therefore, an NIR-emitting nanoparticle with a targeted agent was successfully constructed by the co-assembly method.

To investigate the biological applications of this multivalent supramolecular aggregate, the cell imaging ability of this NIR emission nanoparticle was further evaluated. Figure S17 shows the fluorescence confocal microscopic images of A549 cells (HA receptor over-expressed human lung adenocarcinoma cancer cells) after treatment with TPA/CB[8]/SiR/HA. Obviously, the multivalent supramolecular aggregate exhibited a red luminescence property, manifesting that this TPA/CB[8]/SiR/HA aggregate could serve as an imaging agent. As control experiments, both TPA/CB[8] and TPA/CB[8]/SiR were also treated with A549 cells for 4 h. However, the reference groups gave weak red fluorescence under the same condition. This result may be ascribed to the fact that HA could be readily recognized by the over-expressed hyaluronic acid receptors (such as CD44/RHAMM receptors) on cancer cells[25,27,28] and then facilitated the receptor-mediated endocytosis of the TPA/CB[8]/SiR/HA aggregate into A549 cells. This multivalent aggregate was also added to the normal cells (human embryonic kidney 293T cells) to investigate the cancer cell targeting ability of TPA/CB[8]/SiR/HA. Com-

https://doi.org/10.1021/acsami.1c19698
ACS Appl. Mater. Interfaces 2022, 14, 4417−4422

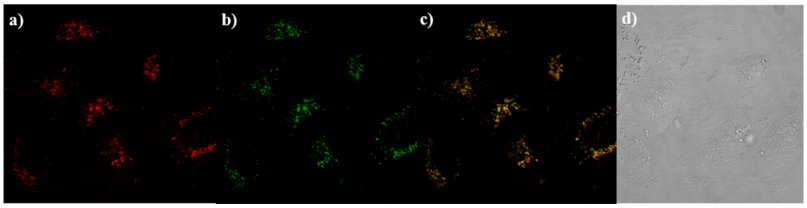

Figure 4. Confocal scanning microscopy image of cancer cells incubated with TPA/CB[8]/SiR/HA and LysoTracker Green (0.01 mM). (a) TPA/CB[8]/SiR/HA (λ_{ex} = 450 nm). (b) LysoTracker Green (λ_{ex} = 488 nm). (c) Merged TPA/CB[8]/SiR/HA and LysoTracker. (d) Bright field ([TPA] = [SiR] = [HA] = 0.01 mM, [CB[8]] = 0.015 mM).

pared with A549 cells, the normal cells showed negligible fluorescence emission indicating that the TPA/CB[8]/SiR/HA hardly entered the normal cells through endocytosis (Figure S18). However, a red luminescence signal was also detected from the control group without HA (TPA/CB[8]/SiR) in 293T cells. Furthermore, when TPA, CB[8], and SiR were added successively into the A549 cells, a fairly weak red fluorescence was observed, indicating that in situ assembly hardly occurred (Figure S19). Therefore, the component of HA in this system endows the assembly with the ability to target cancer cells.

Additionally, we also investigated the possibility of this multivalent assembly as an organelle-targeted imaging agent by confocal laser scanning microscopy. After incubation with NIR nanoparticles, DAPI (the nuclei dye), LysoTracker Green (a lysosome tracker), or MitoTracker Green (a mitochondrion tracker) was also added to cells to investigate the subcellular location of these nanoparticles. Judging from the merged yellow dyeing sites of the red multivalent aggregate and green LysoTracker (Figure 4), TPA/CB[8]/SiR/HA and LysoTracker Green were in good co-localization, indicating that the nanoparticles showed good ability to target lysosome in A549 cells. In sharp contrast, these NIR nanoparticles rarely gave a co-localized signal with DAPI or MitoTracker green (Figures S20−S21), indicating that the aggregate hardly entered the nuclei or mitochondrion. However, the conjugates (TPA/CB[8] or TPA/CB[8]/SiR) without HA could co-localize with MitoTracker Green (Figure S22), manifesting that these conjugates could enter the mitochondrion. Thus, the component of HA in this aggregate endows the assembly with the ability to target lysosome. Consequently, these results jointly indicated that this artificial nanoparticle with NIR emission could serve as a nanoplatform for cancer targeted imaging.

CONCLUSIONS

In conclusion, a targeted near-infrared supramolecular aggregate was successfully fabricated by a multivalent supramolecular assembly strategy. In this aggregate, the tripaddle hexacationic TPA was selected as a guest molecule with weak luminescence, which interacted with CB[8] to form a network-like multivalent aggregate and then induced red emission at 650 nm. Noticeably, such organic two-dimensional network-like conjugate could co-assemble with the energy acceptor SiR, leading to a further red shift of the NIR emission to 675 nm via an intermolecular energy transfer pathway and giving an efficiency up to 69%. Moreover, the artificial conjugate was further transformed to be an NIR emission nanoparticle by second assembly with the cancer cell targeting agent HA. Furthermore, the obtained multivalent supramolecular aggregate with NIR fluorescence emission exhibited lysosome-targeted imaging abilities, which provides a convenient strategy for NIR targeted cell imaging.

ASSOCIATED CONTENT

Supporting Information

The Supporting Information is available free of charge at https://pubs.acs.org/doi/10.1021/acsami.1c19698.

Additional experiment details and methods; synthetic route of TPA; NMR and MS data; DLS and zeta potential data; fluorescence spectra; TEM and EDX images; and confocal scanning microscopy images (PDF)

AUTHOR INFORMATION

Corresponding Author

Yu Liu − *College of Chemistry, State Key Laboratory of Elemento-Organic Chemistry, Nankai University, Tianjin 300071, P.R. China;* orcid.org/0000-0001-8723-1896; Email: yuliu@nankai.edu.cn

Authors

Jie Yu − *College of Chemistry, State Key Laboratory of Elemento-Organic Chemistry, Nankai University, Tianjin 300071, P.R. China*

Hui Wang − *College of Chemistry, State Key Laboratory of Elemento-Organic Chemistry, Nankai University, Tianjin 300071, P.R. China*

Xianyin Dai − *College of Chemistry, State Key Laboratory of Elemento-Organic Chemistry, Nankai University, Tianjin 300071, P.R. China*

Yong Chen − *College of Chemistry, State Key Laboratory of Elemento-Organic Chemistry, Nankai University, Tianjin 300071, P.R. China*

Complete contact information is available at: https://pubs.acs.org/10.1021/acsami.1c19698

Author Contributions

J.Y., H.W., and X.Y.D. synthesized the compounds and performed experiments. J.Y. collected data, summarized, and wrote the work. The project was edited and supervised by Y.C. and Y.L.

Funding

This work supported by the National Natural Science Foundation of China (NNSFC) (grant nos. 22131008 and 21971127) and Hunan Provincial Natural Science Foundation of China (project no. 2020JJ5158).

Notes

The authors declare no competing financial interest.

■ ACKNOWLEDGMENTS

We thank the National Natural Science Foundation of China (NNSFC) (grant nos. 22131008 and 21971127) and Hunan Provincial Natural Science Foundation of China (project no. 2020JJ5158) for financial support.

■ REFERENCES

(1) Ye, M.; Wang, X.; Tang, J.; Guo, Z.; Shen, Y.; Tian, H.; Zhu, W.-H. Dual-Channel NIR Activatable Theranostic Prodrug for in vivo Spatiotemporal Tracking Thiol-Triggered Chemotherapy. *Chem. Sci.* **2016**, *7*, 4958−4965.
(2) Liu, C.; Wang, X.; Liu, J.; Yue, Q.; Chen, S.; Lam, J. W. Y.; Luo, L.; Tang, B. Z. Near-infrared AIE Dots with Chemiluminescence for Deep-tissue Imaging. *Adv. Mater.* **2020**, *32*, 2004685.
(3) Kang, M.; Zhou, C.; Wu, S.; Yu, B.; Zhang, Z.; Song, N.; Lee, M. M. S.; Xu, W.; Xu, F.-J.; Wang, D.; Wang, L.; Tang, B. Z. Evaluation of Structure-function Relationships of Aggregation-Induced Emission Luminogens for Simultaneous Dual Applications of Specific Discrimination and Efficient Photodynamic Killing of Gram-positive Bacteria. *J. Am. Chem. Soc.* **2019**, *141*, 16781−16789.
(4) Woo, S.-J.; Park, S.; Jeong, J.-E.; Hong, Y.; Ku, M.; Kim, B. Y.; Jang, I. H.; Heo, S. C.; Wang, T.; Kim, K. H.; Yang, J.; Kim, J. H.; Woo, H. Y. Synthesis and Characterization of Water-soluble Conjugated Oligoelectrolytes for Near-infrared Fluorescence Biological Imaging. *ACS Appl. Mater. Interfaces* **2016**, *8*, 15937−15947.
(5) Yu, Q.; Zhang, B.; Zhang, Y.-M.; Liu, Y.-H.; Liu, Y. Actin Cytoskeleton-disrupting and Magnetic Field-responsive Multivalent Supramolecular Assemblies for Efficient Cancer Therapy. *ACS Appl. Mater. Interfaces* **2020**, *12*, 13709−13717.
(6) Harada, A.; Takashima, Y.; Nakahata, M. Supramolecular Polymeric Materials via Cyclodextrin-guest Interactions. *Acc. Chem. Res.* **2014**, *47*, 2128−2140.
(7) Baldini, L.; Casnati, A.; Sansone, F.; Ungaro, R. Calixarene-based Multivalent Ligands. *Chem. Soc. Rev.* **2007**, *36*, 254−266.
(8) Appel, E. A.; Biedermann, F.; Rauwald, U.; Jones, S. T.; Zayed, J. M.; Scherman, O. A. Supramolecular Cross-linked Networks via Host-guest Complexation with Cucurbit[8]uril. *J. Am. Chem. Soc.* **2010**, *132*, 14251−14260.
(9) Cooper, C. B.; Kang, J.; Yin, Y.; Yu, Z.; Wu, H.-C.; Nikzad, S.; Ochiai, Y.; Yan, H.; Cai, W.; Bao, Z. Multivalent Assembly of Flexible Polymer Chains into Supramolecular Nanofibers. *J. Am. Chem. Soc.* **2020**, *142*, 16814−16824.
(10) Xu, Z.; Jia, S.; Wang, W.; Yuan, Z.; Ravoo, B. J.; Guo, D.-S. Heteromultivalent Peptide Recognition by Co-assembly of Cyclodextrin and Calixarene Amphiphiles Enables Inhibition of Amyloid Fibrillation. *Nat. Chem.* **2019**, *11*, 86−93.
(11) Li, J.-J.; Zhang, H.-Y.; Liu, G.; Dai, X.; Chen, L.; Liu, Y. Photocontrolled Light-Harvesting Supramolecular Assembly Based on Aggregation-induced Excimer Emission. *Adv. Optical Mater.* **2021**, *9*, 2001702.
(12) Shen, F.-F.; Chen, Y.; Dai, X.; Zhang, H.-Y.; Zhang, B.; Liu, Y.; Liu, Y. Purely Organic Light-harvesting Phosphorescence Energy Transfer by β-cyclodextrin Pseudorotaxane for Mitochondria Targeted Imaging. *Chem. Sci.* **2021**, *12*, 1851−1857.
(13) Yang, X.; Wang, R.; Kermagoret, A.; Bardelang, D. Oligomeric Cucurbituril Complexes: From Peculiar Assemblies to Emerging Applications. *Angew. Chem., Int. Ed.* **2020**, *59*, 21280−21292.
(14) Bhaumik, S. K.; Biswas, R.; Banerjee, S. Cucurbituril Based Luminescent Materials in Aqueous Media and Solid State. *Chem. − Asian J.* **2021**, *16*, 2195−2210.
(15) Xu, D.-A.; Zhou, Q.-Y.; Dai, X. Y.; Ma, X.-K.; Zhang, Y.-M.; Xu, X. F.; Liu, Y. Cucurbit[8]uril-mediated Phosphorescent Supramolecular Foldamer for Antibiotics Sensing in Water and Cells. *Chin. Chem. Lett.* **2021**, DOI: 10.1016/j.cclet.2021.08.001.
(16) Ma, X.-K.; Liu, Y. Supramolecular Purely Organic Room-temperature Phosphorescence. *Acc. Chem. Res.* **2021**, *54*, 3403−3414.
(17) Wang, J.; Huang, Z.; Ma, X.; Tian, H. Visible-light-excited Room-temperature Phosphorescence in Water by Cucurbit[8]uril-mediated Supramolecular Assembly. *Angew. Chem., Int. Ed.* **2020**, *59*, 9928−9933.
(18) Yu, H.-J.; Zhou, Q.; Dai, X.; Shen, F.-F.; Zhang, Y.-M.; Xu, X.; Liu, Y. Photooxidation-driven Purely Organic Room-temperature Phosphorescent Lysosome-targeted Imaging. *J. Am. Chem. Soc.* **2021**, *143*, 13887−13894.
(19) Ni, X.-L.; Chen, S.; Tao, Z. Facile Cucurbit[8]uril-based Supramolecular Approach to Fabricate Tunable Luminescent Materials in Aqueous Solution. *J. Am. Chem. Soc.* **2016**, *138*, 6177−6183.
(20) Wu, G.; Szabó, I.; Rosta, E.; Scherman, O. A. Cucurbit[8]uril-mediated Pseudo[2,3] rotaxanes. *Chem. Commun.* **2019**, *55*, 13227−13230.
(21) Kim, H.-J.; Nandajan, P. C.; Gierschner, J.; Park, S. Y. Light-harvesting Fluorescent Supramolecular Block Copolymers Based on Cyanostilbene Derivatives and Cucurbit[8]urils in Aqueous Solution. *Adv. Funct. Mater.* **2018**, *28*, 1705141.
(22) Jiang, T.; Qu, G.; Wang, J.; Ma, X.; Tian, H. Cucurbiturils Brighten Au nanoclusters in Water. *Chem. Sci.* **2020**, *11*, 3531−3537.
(23) Chen, X.-M.; Chen, Y.; Yu, Q.; Gu, B.-H.; Liu, Y. Supramolecular Assemblies with Near-infrared Emission Mediated in Two Stages by Cucurbituril and Amphiphilic Calixarene for Lysosome-targeted Cell Imaging. *Angew. Chem., Int. Ed.* **2018**, *57*, 12519−12523.
(24) Shen, F.-F.; Chen, Y.; Xu, X.; Yu, H.-J.; Wang, H.; Liu, Y. Supramolecular Assembly with Near-infrared Emission for Two-photon Mitochondrial Targeted Imaging. *Small* **2021**, *17*, 2101185.
(25) Sun, C.; Wang, Z.; Yue, L.; Huang, Q.; Cheng, Q.; Wang, R. Supramolecular Induction of Mitochondrial Aggregation and Fusion. *J. Am. Chem. Soc.* **2020**, *142*, 16523−16527.
(26) Yu, J.; Zhang, Y.-H.; Chen, F.; Xiao, S.; Li, L. White-Light Emission System based on Cyclodextrin/Surfactant Supramolecular Assembly. *Dyes Pigm.* **2020**, *183*, 108748.
(27) Kim, H.; Shin, M.; Han, S.; Kwon, W.; Hahn, S. K. Hyaluronic Acid Derivatives for Translational Medicines. *Biomacromolecules* **2019**, *20*, 2889−2903.
(28) Park, K. M.; Yang, J.-A.; Jung, H.; Yeom, J.; Park, J. S.; Park, K.-H.; Hoffman, A. S.; Hahn, S. K.; Kim, K. In Situ Supramolecular Assembly and Modular Modification of Hyaluronic Acid Hydrogels for 3D Cellular Engineering. *ACS Nano* **2012**, *6*, 2960−2968.

https://doi.org/10.1021/acsami.1c19698
ACS Appl. Mater. Interfaces 2022, 14, 4417−4422